communications earth & environment

ARTICLE

https://doi.org/10.1038/s43247-021-00325-1 OPEN

Asynchronous responses of aquatic ecosystems to hydroclimatic forcing on the Tibetan Plateau

Bernhard Aichner [1,2]✉, Bernd Wünnemann [3,4], Alice Callegaro[5], Marcel T. J. van der Meer [6], Dada Yan[3,4], Yongzhan Zhang[7], Carlo Barbante [5,8] & Dirk Sachse [9]

High-altitude ecosystems react sensitively to hydroclimatic triggers. Here we evaluated the ecological and hydrological changes in a glacier-influenced lake (Hala Hu, China) since the last glacial. Rapid fluctuations of aquatic biomarker concentrations, ratios, and hydrogen isotope values, from 15 to 14,000 and 8 to 5000 years before present, provided evidence for aquatic regime shifts and changes in lake hydrology. In contrast, most negative hydrogen isotope values of terrestrial biomarkers were observed between 9 and 7,000 years before present. This shows that shifts of vapour sources and increased precipitation amounts were not relevant drivers behind ecosystem changes in the studied lake. Instead, receding glaciers and increased meltwater discharge, driven by higher temperatures, caused the pronounced ecological responses. The shifts within phytoplankton communities in the Late Glacial and mid Holocene illustrate the vulnerability of comparable ecosystems to climatic and hydrological changes. This is relevant to assess future ecological responses to global warming.

[1] Institute of Freshwater Ecology and Inland Fisheries, Müggelseedamm 301, 12587 Berlin, Germany. [2] Institute of Geosciences, University of Potsdam, Karl-Liebknecht-Str.24-24, 14476 Potsdam-Golm, Germany. [3] Faculty of Geosciences and Environmental Engineering, Southwest Jiaotong University, Xi'an Rd. 999, 611756 Chengdu, China. [4] Institute of Geographical Sciences, Freie Universität Berlin, Malteserstr. 74-100, 12249 Berlin, Germany. [5] Department of Environmental Sciences, Informatics and Statistics, Ca' Foscari University of Venice, 30172 Venice, Italy. [6] NIOZ Royal Netherlands Institute for Sea Research, Marine Microbiology and Biogeochemistry Department, PO Box 59, 1790AB Den Burg, Netherlands. [7] School of Geography and Ocean Science, Nanjing University, Xianlin Ave. 163, 210093 Nanjing, China. [8] Institute of Polar Sciences—CNR, 30172 Venice, Italy. [9] Helmholtz Centre Potsdam, GFZ German Research Centre for Geosciences, Section 4.6 Geomorphology, Organic Surface Geochemistry Lab, 14473 Potsdam, Germany.
✉email: bernhard.aichner@gmx.de

Ecosystems that are known to react specifically sensitive to climatic changes include those located in mountainous regions[1]. This is even more the case for areas in the confluence zone of atmospheric circulation systems, for example the Tibetan Plateau (TP), which is under influence of both Asian monsoons and westerlies[2–4]. Accordingly, compelling efforts have been undertaken in the last decades to understand the mechanisms controlling the spatial patterns of the TPs ecosystems responses to Northern Hemispheric climatic triggers on different time scales[5–9].

The TP contains ca. 740 lakes with an area >1 km^2 [10], often surrounded by glaciated areas, which provide an enormous source for paleoclimatic archives[11,12]. Despite an increasing number of studies, aspects such as time succession of humidity and temperature and interplay between the Asian monsoon branches and westerlies are still debated[13–16]. Age-model uncertainties and complex control mechanisms on proxies further complicate data interpretation and integration[17–20]. Another challenge is the linkage between proxies that integrate whole catchment processes and their superior hydroclimatic drivers[21], such as changes in atmospheric circulation and precipitation regimes.

Hala Hu is a lake located along the transitional zone between East Asian Summer Monsoon (EASM) and westerlies influence. Several sediment cores have been extensively investigated in terms of catchment and sedimentological processes[9,22–24]. Environmental factors such as present-day seasonal ecosystem dynamics and past lake level changes are well understood. However, inferences on hydrology are based on proxies that integrate whole catchment processes only. Moreover, there is a lack of data with the potential to directly reveal initial hydroclimatic triggers i.e., past changes in monsoonal intensity and vapour source. Further, analysis of biological responses is limited to ostracod assemblages and the distributions of massive algal layers, which were used as markers of changes in water depth in three sediment cores[22,23].

The high organic carbon content makes the lake a promising target for organic geochemical analysis. Aquatic and terrestrial lipid components have the potential to reveal details about both hydroclimatic triggers and ecological responses through the characterization of contributors to the sedimentary organic carbon pool and their hydrogen isotopic signatures[25,26]. We, therefore, analyzed the concentrations of different aquatic and terrestrial biomarker groups and their δD values to investigate: (a) the dynamics of shifting atmospheric circulation systems; and (b) the time succession of ecological responses in the lake and its catchment. The overall aim is to evaluate glacial to interglacial hydroclimatic dynamics and ecosystem responses in a glacier-influenced high-altitude lacustrine ecosystem, representative of the TP.

Study site

Hala Hu is a closed lake basin located in the Qilian Mountains at the northern margin of the TP (ca. 97.24–97.47°E, 38.12–38.25°N, 4,078 m above sea level; Fig. 1). With a surface area of 590 km^2, the lake has a catchment of 4,690 km^2, which is bordered by the surrounding mountain ranges with peaks partly exceeding 5,000 m altitude and glaciers reaching down to 4,600 m altitude at present. It is a saline lake (17–19 psu) with seasonal changes of electric conductivity due to glacial meltwater influence in the summers. In the lake, an algal bloom develops during the summer months in 25–32 m water depth. This leads to oxygen oversaturation in these depths and oxygen depletion to anoxic conditions below[22]. According to the reconstructions based on ostracod assemblages in three cores, the water level was ca. 50–55 m lower than present in the glacial period and rose rapidly between ca. 12 and 10 ka cal BP, while the Holocene was characterized by multiple rapid and short-time lake trans- and regressions, with highest stands during the mid Holocene, ca 8−6 ka cal BP[9,23].

Based on the data from the nearest meteorological station at Delingha (90 km south) and the extrapolation of data to higher altitudes, the mean annual temperature, and precipitation at Hala Hu have been estimated to be −1.5 °C and 228 mm, respectively[22]. Evaporation in the wider region exceeds 1000 mm[9]. Modern precipitation accounts for ca. 60% of the water supply to the lake, the other ca. 40% is provided by glacial meltwater, a ratio which was most likely much different in the past[23]. The vegetation in the lower altitudes of the catchment area is characterized by sparse alpine meadows and the absence of trees.

Results and discussion

Concentrations and sources of organic compounds

Mid- and long-chain n-alkanes. Throughout most sections, the biomarker composition of the Hala Hu record is dominated by long-chain *n*-alkanes (Fig. 2a). In most samples, concentrations were highest for nC_{31} (ca 5–35 µg/g d.w.) and decreasing with chain-length (Supplementary Fig. S3–1). Generally, the concentrations were low in the glacial period, and increased between ca. 10 and 8 ka cal BP, while gradually decreasing after ca. 5 ka cal BP. These alkanes can be attributed to vascular higher plants from the lake catchment[27], which is characterized by alpine meadows. Mid-chain nC_{23} and nC_{25}-alkanes are frequently attributed to aquatic macrophytes[28]. However, *n*-alkane patterns of aquatic and terrestrial plants overlap. Moreover, we consider the contribution from macrophyte to the sedimentary *n*-alkane pool at the coring location to be minor, because of the specific *n*-alkane pattern of the samples, the overall low concentrations of mid-chain *n*-alkanes, and the deep water depth of the core site. An exception is a section in the core dated to ca. 15–14 ka cal BP, that has concentrations from ca. 20 up to 50 µg/g d.w. for individual mid-chain *n*-alkanes (Fig. 2a). This can be explained by enhanced contribution from submerged aquatic plants[29] when the lake level was much lower than present[9,23]. Alternatively, a contribution from other mid-chain producers, such as *Sphagnum* species[30,31], is possible during phases of lake regression and the potential formation of peatlands around the lake shore.

Algal biomarkers. Aside from *n*-alkanes, a range of compounds of mostly aquatic origin can be identified in the aliphatic and ketone fraction of the sediment extracts. Unsaturated mid-chain alkenes $nC_{21:1}$, $nC_{23:1}$, $nC_{25:1}$, and $nC_{27:1}$ were abundant in traces in large parts of the core, but exhibit very high concentrations (>100 µg/g d.w.) in the glacial period in a single sample at 17.5 ka cal BP and between 15 and 14 ka cal BP. Relatively high concentrations up to 25 µg/d.w. were also observed in the mid-Holocene sequence from ca. 9 to 5 ka cal BP (Fig. 2b). The origin of those compounds is not fully resolved and so far *n*-alkenes have not been detected in samples from aquatic and terrestrial vascular plants on the TP. However, algae such as eustigmatophytes and chlorophytes have been suggested as possible precursors in the open freshwater Lake Lugu, southeastern TP[32], and in Lake Challa, eastern Africa[33,34]. Therefore, we consider phytoplankton as the most likely source of those compounds in Hala Hu.

It is notable that different *n*-alkene distribution patterns are visible throughout the core, with a predominance of $nC_{27:1}$ and $nC_{25:1}$ in the mid-Holocene section and $nC_{23:1}$ and $nC_{25:1}$ in other core sections (Supplementary Fig. S3–1). This indicates either different source organisms for at least $nC_{23:1}$ compared to $nC_{27:1}$

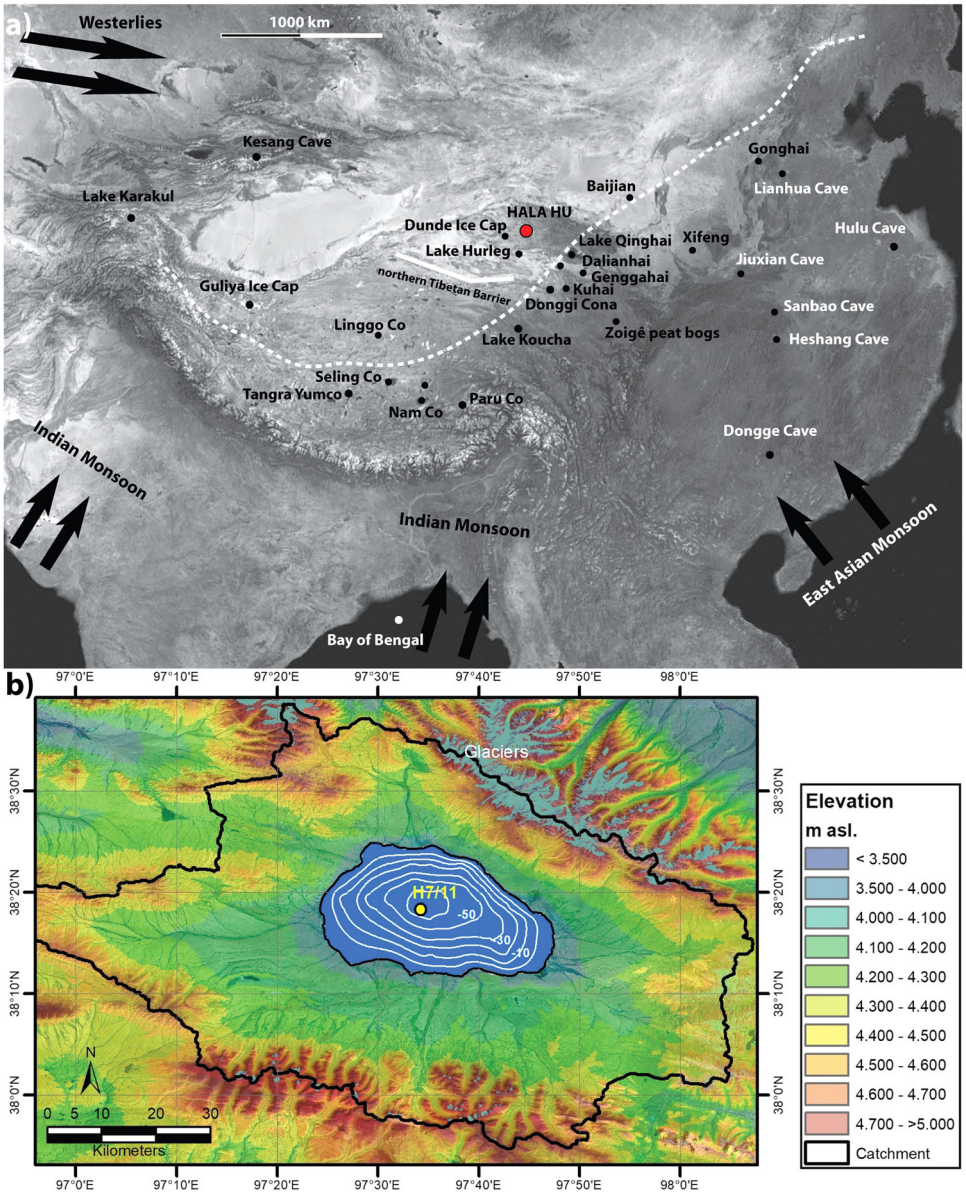

Fig. 1 Study site. a Location of Hala Hu and regional paleorecords as mentioned in the text. Dashed white line indicates approximate boundary zone of present day ASM influence. Northern Tibetan Barrier is the proposed maximum extent of mid-Holocene monsoon influence[102]. **b** Hala Hu and catchment with coring location of H7 and H11[22].

(supported by more depleted δD-values, see below and Supplementary Fig. S3–3) or a change towards the synthesis of longer chain-lengths by the same source organisms, triggered by changing environmental conditions.

The C_{20}-highly branched isoprenoid (HBI) compound is another observed phytoplankton biomarker, which is widely absent in the glacial sequences but shows traces throughout the Holocene with peak abundances (up to 30 µg/g d.w) in the mid-Holocene (8−5 ka cal BP; Fig. 2b). As often been found in cyanobacterial and algal mats (e.g.,[35–37]), it has recently been assigned as a trophic indicator derived from diatoms in lake systems[38].

Other observed biomarkers of algal origin are alkenones, which are primarily produced by haptophytes, even though a variety of species are possible precursors[39,40] The summed concentrations of C_{37}-, C_{38}-, and C_{39}-compounds were low (<50 ng/g d.w.) in most samples from the glacial sections of the core, but increasing after ca. 12 ka cal BP and reaching peak abundances in the mid-Holocene (>300 ng/g d.w.; ca. 7.8–6.3 ka cal BP) (Fig. 2b). Here, the di- and tri-unsaturated homologues of all chain lengths appear to elute as peaks undisturbed by contamination, while the tetra-unsaturated alkenones show co-elution with a fatty acid ethyl ester (FAEE) at least for the C_{37}-compound.

Pentamethylicosane (PMI) is a compound that was detected in most samples in minor concentrations (<100 ng/g d.w.), but shows enhanced concentrations (>400 ng/g d.w.) during an episode in the glacial period (ca 16.6−14 ka cal BP) and during the late Holocene (4.5 ka cal BP to present). This compound has been assigned to microorganisms, i.e bacteria and archaea, often related to the methane cycle[41–44].

Fire markers. Another analyzed biomarker group, anhydrous sugars levoglucosan (L), galactosan (G), and mannosan (M) are generated by combustion and pyrolysis of cellulose and hemicellulose, thus, are often referenced as "pyromarkers" or "firemarkers"[45–47]. They occur in low concentrations (<40 µg/g

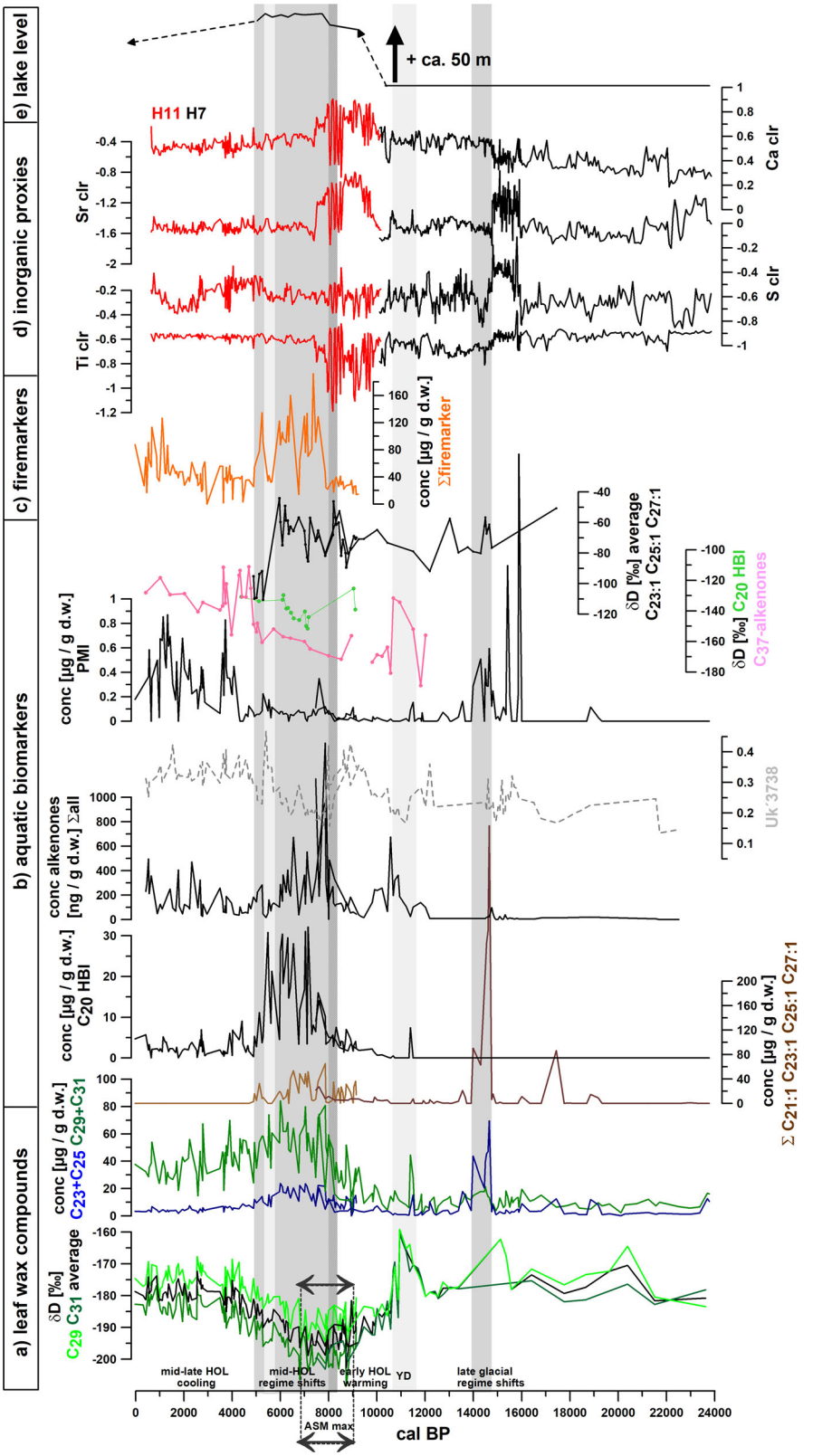

Fig. 2 Summary of measured proxy parameters in cores H7 and H11 (overlap 7.4−9.1 kyrs BP). a δD values and concentrations of mid- and long-chain *n*-alkanes. Arrows (ASM) indicate the maximum strength of the summer monsoon over Asia. **b** Concentrations of aquatic biomarkers (C_{20}-HBI, alkenones, *n*-alkenes) and of microbial derived PMI; alkenone index (Uk'_{37}) and C_{37}-alkenone δD values. **c** Concentrations of firemarkers (ΣM, L, G). **d** Titanium, sulfur, strontium, and calcium contents from XRF-scanning[22,23]. **e** Lake level reconstructed from ostracod assemblages[9]. Dark dashed interval 8.4−8.0 kyrs BP indicates mass flow layer. Light and medium grey shaded areas mark episodes of late glacial and mid-Holocene regime shifts within the aquatic ecosystem.

d.w.) during the early Holocene, but above average concentrations during the mid-Holocene (ca 8–5 ka cal BP), reaching peak values up to 170 µg/g d.w. The concentrations rapidly decrease and then gradually increase to intermediate abundances (ca 80 µg/g d.w.) during the late Holocene (Fig. 2c).

Slightly different trends and lower concentration values of M and G compared to L (Supplementary Fig. S3–1) can be attributed to their different thermal stabilities and consequently much easier degradations of M and G, which derive from hemicellulose[48,49]. The mechanisms behind source to sink dynamics of pyromarkers are not fully understood yet but transport via both aerosols and fluvial organic matter seems important[47]. For an in-depth interpretation of the pyromarker data, other related proxies such as polycyclic aromatic hydrocarbons (PAHs), black carbon, and pollen are required, together with the fire records from other surrounding lacustrine systems. Nevertheless, the rapid mid-Holocene increase of firemarker concentrations at Hala Hu is likely not only caused by the increase of supraregional wildfires triggered by high temperatures, but also due to enhanced fluvial influx to the lake due to strengthened glacial melt during this period.

Ecological inferences. The overall succession, i.e., appearances and disappearances of different biomarker groups indicate the expansion and regression of terrestrial vegetation and aquatic organisms throughout the studied 24 ka. The pronounced regime shifts within the lake ecosystem are remarkable, first during a ca. 1000 year episode in the glacial period (ca. 15−14 ka cal BP), which shows a strong expansion of aquatic organisms and eventually influence of *Sphagnum* species. Further succession of phytoplankton markers started with a first phase of alkenones, appearing from ca. 13–10 ka cal BP, with peak concentration at around 11 ka cal BP. The Holocene is characterized by variable concentrations of all aquatic biomarker groups, that show a clear maximum, starting right above a ca. 15 cm thick mass flow disturbance layer (ca. 8.4−8.0 ka cal BP; Fig. 2) and terminating at ca 5 ka cal BP. Synchronously, some biomarker groups show changes in relative abundances of single compounds (e.g., $C_{23:1}$ vs. $C_{27:1}$-alkenes, $\%C_{37:4}$-alkenones and $\Sigma C_{37}/\Sigma C_{38}$ alkenones; Fig. 2b, Supplementary Fig. S3–1), which suggests shifts in communities of precursor organisms. These data give evidence of an ecological optimum between 8 and 5 ka cal BP. This episode was characterized by an overall higher and more diverse aquatic productivity compared to present-day condition, by the expansion of terrestrial vegetation, and by the increased influx of firemarkers.

Hydroclimatic trends throughout the past 24 ka

Catchment hydrology. As the source of terrestrial long-chain *n*-alkanes is limited to alpine grasses, their δD values represent mainly a growing season (i.e., summer) moisture signal. An influence of meltwater (snow, glaciers, and thawing permafrost) is debated as an additional water source, possibly incorporating a more negative isotope signal during leaf wax synthesis, especially at locations with a short growing season[21,50,51]. The δD data since 24 ka cal BP demonstrate more negative values between ca 11 and 5 ka cal BP (minimum from ca. 9–7 ka cal BP) and further indicate a positive shift at around 11 ka cal BP. The latter is -within the margin of age-model uncertainties- probably associated with the Younger Dryas (YD).

In general, the data resembles the isotopic trends observed in other locations in the Asian monsoon realm and adjacent areas, derived from multiple archives and proxies such as speleothem $\delta^{18}O$ and sedimentary leaf wax δD (Fig. 3). While age-model uncertainties often prevent the interpretation of short-term events and local effects and influence the amplitude of the recorded signal, the overall shift of δD values from high (Late Glacial) to low (Holocene) is observable in most sedimentary leaf wax records from the TP[52], the Indian Monsoonal Realm/Bay of Bengal[53], and in Central Asia[50] (Fig. 3d, f). The available leaf wax δD records next to Hala Hu are from Lake Hurleg and Lake Qinghai, both less than 300 km south and southeast to Hala Hu, respectively (Fig. 1a). Lake Hurleg shows the most negative δD_{nC31} values of the record between ca. 9 and 8 ka cal BP[54] (Fig. 3e). Data from Lake Qinghai show depletion of δD values of C_{28}-fatty acids earlier, i.e., already during the Late Glacial[55,56]. Speleothem records show slight differences in detail, but in general reveal the most negative $\delta^{18}O$ values at around 8 ka cal BP[57–59] (Fig. 3c, d).

The pattern with lower δD-values during the early and mid-Holocene has frequently been explained by intensified monsoon (e.g.,[55,60], and refs. in Fig. 3). While this is plausible, the extent to which enhanced precipitation amounts, temperature effects, or change of vapour sources contribute to local isotopic signals in sediments and speleothems is still under debate[20,58]. Modern seasonal data from the Qilian Mountains suggest a pattern of temperature control and no amount effect on precipitation isotopes, i.e., relatively high modern isotopic values during the summer season[61]. On longer time-scales, expected temperature effects run opposite to the observed lower/higher δD values during the mid-Holocene/YD, respectively. An increase of precipitation amounts could possibly contribute to a more negative isotopic signal in summers. Indeed, the episode of most negative δD values corresponds to lake level highstands in more eastern locations, such as Lake Baijian[62]. More likely, we hypothesize that the isotope signal is driven by changes of vapour sources, induced by the movement and tilt of the jet-stream during the Holocene[63], or by coupling processes to upstream regions such as the tropical monsoon realms[58,64] In any case, shifts of the boundaries between monsoonal and westerly air masses are the most likely explanation for the observed trend of long-chain *n*-alkane δD-values in the Hala Hu sediments.

Lake isotope hydrology. To infer hydrological states of lakes, the hydrogen isotopic compositions of aquatic organisms have frequently been used. Biomarkers derived from aquatic macrophytes, such as nC_{23}, appear to be good recorders of lake water δD[65]. However, in Hala Hu they were abundant only in low concentrations and therefore most likely mixed with terrestrial alkanes. Exceptional is the period ca. 15–14 ka cal BP. Here, the highly concentrated nC_{23} exhibited highly variable δD values, averaging ca. 70‰ higher compared to the terrestrial compounds (Supplementary Fig. S3–3). This possibly indicates a mixed origin of compounds from macrophytes and *Sphagnum* sources, both of which have grown under uptake of lake and wetland water that has undergone evaporative D-enrichment. The drivers behind δD values of algal markers have been relatively well-investigated for alkenones but comparably little data exist for mid-chain *n*-alkenes and HBIs. A recent transect study has shown that C_{20}-HBIs potentially track lake water δD[66]. Alkenones appear to record the δD values of the ambient water, but with strong potential effects of salinity and species associations[67–73].

In Hala Hu, δD values of all three analyzed biomarker groups (alkenones, alkenes, and HBIs) show tendencies towards higher values from the early to the mid and late Holocene, mostly reflecting the trend as derived from terrestrial compounds (Fig. 2b and Supplementary Fig. S3–3). Here, C_{20}-HBIs are slightly D-enriched compared to C_{37}-alkenones, and *n*-alkenes show further 50–60‰ higher values than those two compounds. The termination of the mid-Holocene is characterized by strong and opposing shifts in δD values of alkenones and *n*-alkenes. Given the succession of climatic, ecological, and hydrological changes,

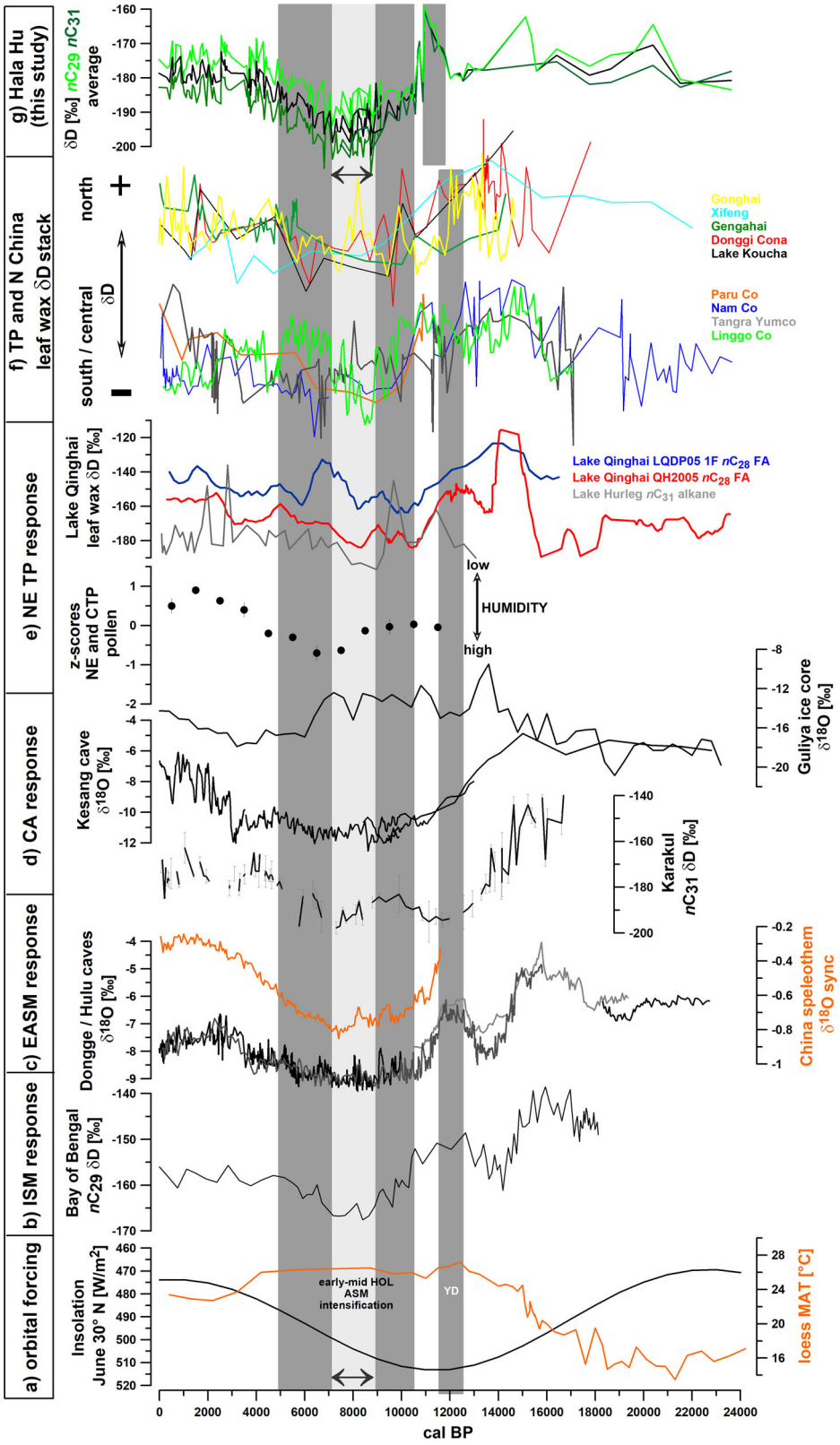

which include cooling and community shifts, these factors are plausible triggers for a ca. 40‰ positive shift in δD values of alkenones after 5 ka cal BP and the general trend towards higher δD values during the late Holocene (Fig. 2b; Supplementary Fig. S3–3). An opposite (i.e., negative) 60‰ shift in δD values of alkenes at ca. 6−5 ka cal BP (Fig. 2b) is more difficult to explain. Similar to alkenones, a change in community compositions of alkene producers can be a relevant factor, since this shift is mostly visible in nC$_{23:1}$ and nC$_{25:1}$, less in nC$_{27:1}$ (Supplementary Fig. S3–3), in agreement with varying nC$_{23:1}$ to nC$_{27:1}$ ratios (Supplementary Fig. S3–1). Considering the present day algal zone at 25–32 m depth[23], migration to different depths as a consequence of the hydrological changes and a related change of source water δD is another possible explanation.

Fig. 3 Comparison with regional hydroclimatic records. a Insolation[103] and GDGT based MAT from the Chinese Loess Plateau[13]. Regional δD records: **b** Indian Summer Monsoon (ISM) influence zone: Bay of Bengal, SO188-342-KL[53]. **c** East Asian Summer Monsoonal (EASM) realm: $\delta^{18}O$ of Dongge and Hulu Cave[104–106] and synthesis record of East China speleothems[59]. **d** Central Asian (CA) response: Lake Karakul nC_{31} δD[50], Kesang Cave speleothem[57], and Guliya ice core $\delta^{18}O$[11]. **e** Northeastern Tibetan responses: vegetation derived from pollen (humidity index from NE and CTP lakes Zoigê peat bog, Dalianhai, Hurleg, Qinghai, Zigetang, Seling Co and Dunde Ice Cap; compiled in[97]. Leaf wax δD of Lake Hurleg[54] and Lake Qinghai[55,56]. **f** Stack plot of normalized δD-values from northern and southern/central TP: Lake Genggahai[54], Xifeng Loess section[107], Lake Gonghai[19], Lake Donggi Cona[108], Lake Koucha[65], Lake Paru Co[60], Nam Co[109], Linggo Co[55]. **g** δD-values of long-chain alkanes in Hala Hu (this study). Dark shaded area: YD and early/mid-Holocene. Light shaded area: most negative δD values in Hala Hu.

In general, both the alkenone and *n*-alkene δD-data pinpoint to a range of ecological and hydrological changes around 6–5 ka cal BP. Further, the alkenones mirror the YD-isotopic signal at around 11 ka cal BP, as observed in the terrestrial long-chain *n*-alkanes (Fig. 2a). The results show the impact of climatic changes on lake ecology and hydrology during these episodes. They further highlight the potential of the applied proxy parameters to integrate and track aquatic community responses.

Alkenone indices. To elucidate the proxy potential of alkenones in the Hala Hu record, we computed multiple common ratios for comparison (Supplement S1–1). The temperature dependency of the degree of unsaturation of alkenones[39] have led to extensive calibration attempts in order to reconstruct water temperatures[74]. While established in the marine realm, numerous indices and calibration-equations have been proposed for lacustrine systems in different regions[75] including China[24,76–84]. All of these studies suggest that the influencing factors on alkenone biosynthesis are complex. Alongside temperature they include the effects of variable salinities and other water chemistry-related parameters, changes in the seasonality of biosynthesis, community shifts and phylogeny of alkenone producers, and their potential relocation and depth migration within lakes.

For this study, we calculated the classic U^k and $U^{k'}$ indices for either C_{37}- or C_{38}-compounds[85,86], hybrid indices based on both the C_{37} and C_{38}-group[80,87], as well as the percentages of C_{37}- and C_{38}- compounds and the ratio $\Sigma C_{37}/\Sigma C_{38}$ (plotted for comparison in Supplementary Fig. S3–2).

The data show comparable trends of all indices which exclude the tetra unsaturated $C_{37:4}$ alkenone, i.e., $U^{k'}_{37}$; U^k_{38}, $U^{k'}_{38}$, and $U^{k'}_{3738}$ (Supplementary Fig. S3–2). The different behaviour of $C_{37:4}$ has been observed previously and was explained by complex influences of salinity and species contribution[67,79,88]. Notable in the Hala Hu record is a negative correlation between $\%C_{37:4}$ and concentrations of terrestrial *n*-alkanes during the Holocene (Fig. 2a and Supplementary Fig. S3–2), which suggests that control mechanisms on $C_{37:4}$ abundances other than temperature are likely. Finally, the calculated $C_{37:4}$ concentrations may be biased by partial co-elution of this compound with FAEE. For this reason, we focus on the indices which exclude $C_{37:4}$ and therefore chose the integrative hybrid index $U^{k'}_{3738}$[87] (Fig. 2b) for further data interpretation.

In general, $U^{k'}_{3738}$ shows relatively low values during the glacial period and the YD, indicating low temperatures. Increasing $U^{k'}_{3738}$ values between ca. 11 and 9 ka cal BP could then be related to warming conditions at the Late Glacial—early Holocene transition.

A reversal to lower values from ca. 9 to 5 ka cal BP would then indicate cooler water temperatures at the location of alkenone synthesis. Those could be explained by glacial freshwater pulses and related cooling of the lake water above the thermocline, as a mid-Holocene lake transgression was inferred from biological and sedimentary proxies[23]. However, most algae within the modern lake are found far below the thermocline, where water temperatures are relatively stable, diminishing the potential influence of water temperature on alkenone parameters.

The integrated results from aquatic biomarkers illustrate the profound effects of rising lake levels and related change in lake water chemistry on phytoplankton communities during the mid-Holocene. It is therefore likely that shifts in alkenone producers rather than temperature changes are the primary cause of the lower $U^{k'}_{3738}$ values between 9 and 5 ka cal BP.

Hydroclimatic inferences. δD values of long-chain *n*-alkanes reflect regional isotope hydrology and hence are considered as a proxy for shifts within the atmospheric circulation system. We, therefore, interpret the most negative δD values of the records, from ca. 9 to 7 ka cal BP, to be associated with changes in moisture source, synchronous with an intensified ASM over Asia. It needs to be highlighted that this inference is independent from the exact origin of vapour transported to the study area during ASM, which possibly includes westerly moisture sources and local convection[20]. Further, the actual increase of precipitation and/or effective moisture in the Hala Hu catchment during this episode were most likely minor.

A YD signal is observable in both terrestrial and aquatic δD values (Fig. 2), indicating an impact of this event on both the catchment and lake hydrology in the Hala Hu region. While an early Holocene warming is probably recorded by the $U^{k'}_{3738}$, there is evidence of strong effects of community shifts during the mid-Holocene (8—ca. 5 ka cal BP). The termination of the mid-Holocene is characterized by multiple hydrological and ecological changes, visible in decreasing aquatic and terrestrial biomarker concentrations and shifts in δD values of aquatic compounds.

Ecological responses to hydroclimatic forcing. The current trophic status of Hala Hu has not been determined by water chemical parameters, but the extensive oxygen supersaturated algal zone above an oxygen zone support mesotrophic conditions. These conditions are reflected by low to average concentrations of phytoplankton biomarkers from the late Holocene to the present (Fig. 2b).

In principle, lakes often achieve alternate steady states, that are ecosystem states where either macrophyte or phytoplankton dominates[89]. This concept was initially proposed for shallow lakes but has been shown to be applicable also for some deeper lakes, in which especially submerged macrophytes have a stabilizing function on ecosystem composition[90,91]. Many lakes on the TP are saline, oligotrophic, and relatively shallow[12]. Due to high insolation and clear water, strong submerged macrophyte growth, often down to significant depths, is very common in Tibetan lakes[29].

To interpret past changes of these conditions from organic geochemical proxy data, transporting mechanisms of biomarkers need to be considered. For example, a survey of surface sediments in Lake Donggi Cona has shown that submerged macrophytes mainly influence the near shore zones, and samples from deeper parts of the lake receive low concentrations of aquatic mid-chain *n*-alkanes[92]. At present, aquatic macrophytes occur at least in the near-shore zones at Hala Hu[23]. The very low concentrations of macrophyte markers (nC_{23} and nC_{25}) can be explained by the

absence of submerged higher plants at the coring location since the early Holocene, but do not allow conclusions about potential abundances at more shallow water depths.

Very different conditions occurred in the glacial period, when a peak of nC_{23} provides evidence for macrophyte expansion during a phase of much lower lake level than present. An increased influence of wetlands and supply of nC_{23} derived from *Sphagnum* sp. is likely and could explain enhanced concentrations of PMI derived from methanogens. Before 15 ka cal BP glaciers extended into the lake, evidenced by the moraine deposits found in the lower part of a core which was obtained near the northwestern shore of Hala Hu[22]. Sr and S contents were high during this period, salinity was likely greater, which is in line with the appearance of the first alkenone producers[23] (Fig. 2b, d). After 15 ka cal BP other phytoplankton- (*n*-alkenes), macrophyte- (alkanes), and microbial markers (PMI) increased synchronously. These data point towards a slightly enhanced nutrient supply and a change in lake water chemistry that is supported by the increased elemental values (Fig. 2d). This first short-term expansion phase of both macrophytes and phytoplankton was associated with a temperature increase at 15 ka cal BP, and likely accompanied by receding glaciers, enhanced freshwater influx, and more favourable conditions for growth in general. This episode is synchronous to Northern Hemispheric warming (Bølling interstadial)[93], but a definite correlation with this event needs to be considered with care, due to age-model uncertainties.

While the exact progression of glacier retreat at surrounding mountains after the ca. 50 m rise of the lake level between ca 12 and 10 ka cal BP remains unknown, multi-proxy data indicate water level fluctuations with episodes of higher lake levels than present during the mid-Holocene from ca. 8 to 6 ka cal BP[9,23]. The combined effects of changes in water chemistry due to glacial meltwater, and higher temperatures probably shifted the lake ecosystem to a more phytoplankton-dominated state. A fertilization effect from either glacial meltwater and/or aerosols is possible and supported by the high firemarker concentrations during the mid-Holocene[47,94]. Suspended sediments transported by glacial meltwater is an important influencing factor in high-altitude lake ecosystems, with effects on both light penetration and nutrient supply, in combination often limiting macrophyte growth[94–96]. Terrestrial biomarkers reached their highest concentrations between ca. 8 and 5 ka cal BP, however their increase and decrease before and after this ecological optimum is more gradual than that of aquatic compounds. We interpret this variability as the result of expansion and regression of grasses in the catchment, driven by the effects of higher temperatures and increase of effective moisture[97] (Fig. 2). Additionally, increased surface runoff derived from melting glaciers could have contributed to the higher influx from terrestrial leaf waxes to the sediments during the mid-Holocene.

There is a considerable lag in the Hala Hu record between the mid-Holocene ecological optimum (characterized by the maximum expansion of alpine grasses and the highest phytoplankton productivity in the lake), and the initial atmospheric forcing (i.e., change of vapour source synchronous to monsoonal intensification). The controlling mechanisms on Holocene vegetation expansion have been debated recently, though there are hints that temperature and temperature-controlled feedback mechanisms are the dominant force on terrestrial ecosystems on the eastern TP[16,18,97]. The Hala Hu data likewise point towards air temperature and the subsequent discharge of glacial meltwater as driving factors of massive ecosystem response in the lake and its catchment.

The termination of a mid-Holocene optimum has been observed in numerous lake sediment, speleothem, and ice core records[6,9,11,13,20,59,97] (Fig. 3). It has been hypothesized that a cooling episode 5–3 ka cal BP, inferred from an Lake Qinghai alkenone record, delayed the population of the north-eastern TP in the late Holocene[78]. We do not see a similar trend in the alkenone indices at Hala Hu, however, we observe regression of grasses, a sharp decrease of aquatic biomarkers concentrations, and shifts in aquatic δD values, all illustrating rapid ecosystem responses to cooler conditions after ca. 5 ka cal BP.

Conclusions

Organic geochemical data from Hala Hu show asynchronous responses of the aquatic and terrestrial ecosystem in the lake and its catchment to hydroclimatic changes. This illustrates the importance of including proxies representative for both biomes in paleolimnological studies, to fully assess linkage and feedback mechanisms between lakes and their catchments.

At first, a succession of phytoplankton and an increase of macrophyte and algal productivity is observed during the late glacial period (15−14 ka cal BP), probably induced by a first freshwater pulse associated with climate warming. A signal of a Younger Dryas cold episode is seen in the isotopic signatures of both terrestrial and aquatic biomarkers, but an ecosystem response is not clearly visible, as aquatic productivity and hence biomarker concentrations were generally low before the onset of the Holocene.

While more negative δD values of terrestrial biomarkers indicate a maximum influence of atmospheric vapour shifts during 9−7 ka cal BP, distinct mid-Holocene aquatic regime shifts and maxima of terrestrial biomarker and firemarker fluxes occurred asynchronously, i.e., between 8 and 5 ka cal BP. These results provide evidence that neither shifts in vapour sources nor increased precipitation amount were the major triggers of ecosystem responses. Instead, increased temperatures during the Holocene optimum, receding glaciers, and consequently increased meltwater discharge into the lake caused the pronounced changes in phytoplankton communities. The termination of the mid-Holocene optimum at Hala Hu is characterized by a gradual decline of terrestrial vegetation and rapid decrease of aquatic biomarker abundances in combination with strong shifts in their δD values, the latter interpreted to indicate pronounced changes in lake hydrology.

The rapid appearances and disappearances of aquatic biomarkers in the Late Glacial and mid-Holocene illustrate the sensitivity of high altitude mountain systems along the modern marginal zone of Asian monsoon influences to climatic changes. Here, independently from monsoonal intensity changes, temperature changes and related meltwater influx have the strongest impact on aquatic communities. This is pivotal when assessing the impact on comparable ecosystems related to expected higher temperatures in the future.

Material and methods

Sediment cores and chronology. As described in detail in[23] two sediment cores H7 and H11 were obtained at the deepest point of Hala Hu (65 m water depth) with a UWITEC piston corer (Fig. 1). The lithology of the core is mainly characterized by finely laminated clayey lake mud, and two silty/clayey sections at ca. 560–525 cm and 460–420 cm depth, respectively. Further, a section consisting of carbonate (dolomite) incorporated with clayey clasts at 240–225 cm depth, equivalent to the phase ca. 8.4–8.0 ka cal BP according to the age-model[9], was interpreted as a result of mass flow event and hence representing older material[22,23].

Radiocarbon ages of 19 samples (bulk organic matter and plant samples) were determined at Poznan Radiocarbon Laboratory, Poland (H7) and BETA Analytical Laboratory, Miami, USA

(H11) (Supplementary Table S2). To establish the age-depth model using Bacon in R[98], seven obtained ages were considered as outliers, and a constant reservoir age of 251 years was used, following the most recent published methodology[9]. The resulting record covers weighted mean ages of 0−9216 cal. years over composite depths of 0−262 cm (core H11), and 7062−24,166 cal. years over composite depths of 200−642 cm (core H7) (Fig. 1).

Analysis. For organic geochemical analysis, a two-phase extraction method was applied by using a Dionex ASE 350. For the first step, dichloromethane (DCM) was used as an extraction solvent while methanol (MeOH) was used for the second step (2 static cycles of 10 min at 100 °C and 1100 psi at each step). The DCM-total lipid extract (TLE) of H7 and H11 samples were split into fractions by using silica-gel columns and hexane (aliphatic fraction), DCM (ketone fraction), and DCM:MeOH 1:1 (alcohol fraction) following the manual solid phase extraction (SPE) protocols described in detail in ref. [99]. The aliphatic fraction was further split chromatographically into a saturated and unsaturated fraction using aluminium-coated silica gel as stationary phase and hexane and DCM as solvents. The MeOH-TLE of H11 samples was dried, water dissolved, and centrifuged before purification with Maxi-Clean C18 columns (W.R. Grace & Co) to additionally obtain monosaccharide-anhydrides (MAs), following the methodology as described in[45]. Concentrations and hydrogen isotopic values of compounds in the saturated aliphatic, unsaturated aliphatic, and ketone fraction were obtained by gas chromatography and isotope ratio mass spectrometry with similar methods as described in refs. [50] and [100] under application of standard measures for quality assurance. As long-chain diols were discovered in some surface sediment samples from different locations in Hala Hu, six alcohol fractions distributed equally across the H11, were also screened but compounds not detected. To analyze δD values in samples with low concentrations of target compounds (i.e., older than 13 ka BP), aliphatic fractions of 3–10 samples have been merged after quantification on the GC and before GC-IRMS analysis. For MA-analysis, IC-MS (ion chromatography-mass spectrometry) methods according to ref. [46] have been applied. A detailed description of the methodology is given in the Supplementary methods S1. All the mentioned lab analyses were conducted in the Organic Surface Geochemistry Lab at GFZ Potsdam, except δD analysis of alkenones and MA quantification, which were conducted at NIOZ and University of Venice, respectively.

Data availability

Data are available at PANGAEA:[101] https://doi.org/10.1594/PANGAEA.933814.

Received: 17 May 2021; Accepted: 26 November 2021;
Published online: 10 January 2022

References

1. Pauli, H. Climate change impacts on high-altitude ecosystems. *J. Mountain Res. Dev.* **36**, 125–126 (2016).
2. An, Z. S. et al. Interplay between the Westerlies and Asian monsoon recorded in Lake Qinghai sediments since 32 ka. *Sci. Rep.* **2**, 619 (2012).
3. Wang, P. X. et al. The global monsoon across time scales: mechanisms and outstanding issues. *Earth-Sci. Rev.* **174**, 84–121 (2017).
4. Chen, F. H. et al. Westerlies Asia and monsoonal Asia: Spatiotemporal differences in climate change and possible mechanisms on decadal to sub-orbital timescales. *Earth-Sci. Rev.* **192**, 337–354 (2019).
5. Morrill, C., Overpeck, J. T. & Cole, J. E. A synthesis of abrupt changes in the Asian summer monsoon since the last deglaciation. *Holocene* **13**, 465–476 (2003).
6. Herzschuh, U. Palaeo-moisture evolution in monsoonal Central Asia during the last 50,000 years. *Quaternary Sci. Rev.* **25**, 163–178 (2006).
7. Ran, M. & Feng, Z. D. Holocene moisture variations across China and driving mechanisms: a synthesis of climatic records. *Quaternary Int.* **313**, 179–193 (2013).
8. Chen, F. H. et al. Climate change, vegetation history, and landscape responses on the Tibetan Plateau during the Holocene: a comprehensive review. *Quaternary Sci. Rev.* **243**, 106444 (2020).
9. Yan, D. D., Wunnemann, B. & Zhang, Y. Z. Late Quaternary lacustrine Ostracoda and their implications for hydro-climatic variation in Northeastern Tibetan Plateau. *Earth-Sci. Rev.* **207**, 103251 (2020).
10. Wan, W. et al. A lake data set for the Tibetan Plateau from the 1960s, 2005, and 2014. *Sci. Data* **3**, 160039 (2016).
11. Thompson, L. G. et al. Holocene Late Pleistocene climatic ice core records from Qinghai-Tibetan Plateau. *Science* **246**, 474–477 (1989).
12. Ma, R. H. et al. China's lakes at present: number, area and spatial distribution. *Sci. China Earth Sci.* **54**, 283–289 (2011).
13. Peterse, F. et al. Decoupled warming and monsoon precipitation in East Asia over the last deglaciation. *Earth Planet Sci. Lett.* **301**, 256–264 (2011).
14. Chen, F. H. et al. Holocene moisture and East Asian summer monsoon evolution in the northeastern Tibetan Plateau recorded by Lake Qinghai and its environs: a review of conflicting proxies. *Quaternary Sci. Rev.* **154**, 111–129 (2016).
15. Zhang, X. J., Jin, L. Y., Chen, J., Lu, H. Y. & Chen, F. H. Lagged response of summer precipitation to insolation forcing on the northeastern Tibetan Plateau during the Holocene. *Clim. Dynam.* **50**, 3117–3129 (2018).
16. Cheng, J. et al. Vegetation feedback causes delayed ecosystem response to East Asian Summer Monsoon Rainfall during the Holocen. *Nat. Commun.* **12**, 1843 (2021).
17. Zhang, J. W. et al. Holocene monsoon climate documented by oxygen and carbon isotopes from lake sediments and peat bogs in China: a review and synthesis. *Quaternary Sci. Rev.* **30**, 1973–1987 (2011).
18. Zhao, Y., Yu, Z. C. & Zhao, W. W. Holocene vegetation and climate histories in the eastern Tibetan Plateau: controls by insolation-driven temperature or monsoon-derived precipitation changes? *Quaternary Sci. Rev.* **30**, 1173–1184 (2011).
19. Rao, Z. G., Li, Y. X., Zhang, J. W., Jia, G. D. & Chen, F. H. Investigating the long-term palaeoclimatic controls on the delta D and delta O-18 of precipitation during the Holocene in the Indian and East Asian monsoonal regions. *Earth-Sci. Rev.* **159**, 292–305 (2016).
20. Wunnemann, B. et al. A 14 ka high-resolution delta O-18 lake record reveals a paradigm shift for the process-based reconstruction of hydroclimate on the northern Tibetan Plateau. *Quaternary Sci. Rev.* **200**, 65–84 (2018).
21. Yan, D. D., Wunnemann, B., Stauch, G., Zhang, Y. Z. & Long, H. Late Quaternary seasonal process variations in lake basins on the NE Tibetan Plateau. *Quaternary Sci. Rev.* **252**, 106736 (2021).
22. Wunnemann, B. et al. Implications of diverse sedimentation patterns in Hala Lake, Qinghai Province, China for reconstructing Late Quaternary climate. *J Paleolimnol* **48**, 725–749 (2012).
23. Yan, D. & Wunnemann, B. Late Quaternary water depth changes in Ha la Lake, northeastern Tibetan Plateau, derived from ostracod assemblages and sediment properties in multiple sediment records. *Quaternary Sci. Rev.* **95**, 95–114 (2014).
24. Wang, Z., Liu, Z. H., Zhang, F., Fu, M. Y. & An, Z. S. A new approach for reconstructing Holocene temperatures from a multi-species long chain alkenone record from Lake Qinghai on the northeastern Tibetan Plateau. *Org. Geochem.* **88**, 50–58 (2015).
25. Castaneda, I. S. & Schouten, S. A review of molecular organic proxies for examining modern and ancient lacustrine environments. *Quaternary Sci. Rev.* **30**, 2851–2891 (2011).
26. Sachse, D. et al. Molecular paleohydrology: interpreting the hydrogen-isotopic composition of lipid biomarkers from photosynthesizing organisms. *Annu. Rev. Earth Planet. Sci.* **40**, 221–249 (2012).
27. Eglinton, G. & Hamilton, R. J. Leaf epicuticular waxes. *Science* **156**, 1322 (1967).
28. Ficken, K. J., Li, B., Swain, D. L. & Eglinton, G. An n-alkane proxy for the sedimentary input of submerged/floating freshwater aquatic macrophytes. *Org. Geochem.* **31**, 745–749 (2000).
29. Aichner, B., Herzschuh, U. & Wilkes, H. Influence of aquatic macrophytes on the stable carbon isotopic signatures of sedimentary organic matter in lakes on the Tibetan Plateau. *Org. Geochem.* **41**, 706–718 (2010).
30. Baas, M., Pancost, R., van Geel, B., Sinninghe & Damsté, J. S. A comparative study of lipids in Sphagnum species. *Org. Geochem.* **31**, 535–541 (2000).
31. Nichols, J. E., Walcott, M., Bradley, R., Pilcher, J. & Huang, Y. Quantitative assessment of precipitation seasonality and summer surface wetness using ombrotrophic sediments from an Arctic Norwegian peatland. *Quaternary Res.* **72**, 443–451 (2017).

32. Zhang, Y. D. et al. Long-chain n-alkenes in recent sediment of Lake Lugu (SW China) and their ecological implications. *Limnologica* **52**, 30–40 (2015).
33. van Bree, L. G. J. et al. Seasonal variability in the abundance and stable carbon-isotopic composition of lipid biomarkers in suspended particulate matter from a stratified equatorial lake (Lake Chala, Kenya/Tanzania): implications for the sedimentary record. *Quaternary Sci. Rev.* **192**, 208–224 (2018).
34. van Bree, L. G. J. et al. Origin and palaeoenvironmental significance of C-25 and C-27 n-alk-1-enes in a 25,000-year lake-sedimentary record from equatorial East Africa. *Geochim. Cosmochim. Acta* **145**, 89–102 (2014).
35. Jaffe, R., Mead, R., Hernandez, M. E., Peralba, M. C. & DiGuida, O. A. Origin and transport of sedimentary organic matter in two subtropical estuaries: a comparative, biomarker-based study. *Org. Geochem.* **32**, 507–526 (2001).
36. Kenig, F. et al. Occurrence and origin of monomethylalkanes, dimethylalkanes, and trimethylalkanes in modern and Holocene cyanobacterial mats from Abu-Dhabi, United-Arab-Emirates. *Geochim. Cosmochim. Acta* **59**, 2999–3015 (1995).
37. Rowland, S. J. & Robson, J. N. The widespread occurrence of highly branched acyclic C-20, C-25 and C-30 hydrocarbons in recent sediments and biota—a review. *Mar. Environ. Res.* **30**, 191–216 (1990).
38. Muschitiello, F., Andersson, A., Wohlfarth, B. & Smittenberg, R. H. The C-20 highly branched isoprenoid biomarker—a new diatom-sourced proxy for summer trophic conditions? *Org. Geochem.* **81**, 27–33 (2015).
39. de Leeuw, J. W., van de Meer, F. W., Rijpstra, W. I. C. & Schenck, P. A. On the occurrence and structural identification of long chain unsaturated ketones and hydrocarbons in sediments. *Phys. Chem. Earth* **12**, 211–217 (1980).
40. Theroux, S., D'Andrea, W. J., Toney, J., Amaral-Zettler, L. & Huang, Y. S. Phylogenetic diversity and evolutionary relatedness of alkenone-producing haptophyte algae in lakes: implications for continental paleotemperature reconstructions. *Earth Planet Sci. Lett.* **300**, 311–320 (2010).
41. Brassell, S. C., Wardroper, A. M. K., Thomson, I. D., Maxwell, J. R. & Eglinton, G. Specific acyclic isoprenoids as biological markers of methanogenic bacteria in marine sediments. *Nature* **290**, 693–696 (1981).
42. Holzer, O., Oro, J. & Tomabene, T. G. Gas chromatography-mass spectrometric analysis of neutral lipids from methanogenic and thermoacidophilic bacteria. *J. Chromatographie A* **186**, 795–809 (1979).
43. Schouten, S., VanderMaarel, M. J. E. C., Huber, R. & Damste, J. S. S. 2,6,10,15,19-Pentamethylicosenes in Methanolobus bombayensis, a marine methanogenic archaeon, and in Methanosarcina mazei. *Org. Geochem.* **26**, 409–414 (1997).
44. Thiel, V. et al. Highly isotopically depleted isoprenoids: molecular markers for ancient methane venting. *Geochim. Cosmochim. Acta* **63**, 3959–3966 (1999).
45. Callegaro, A. et al. Fire, vegetation, and Holocene climate in a southeastern Tibetan lake: a multi-biomarker reconstruction from Paru Co. *Clim. Past* **14**, 1543–1563 (2018).
46. Kirchgeorg, T., Schupbach, S., Kehrwald, N., McWethy, D. B. & Barbante, C. Method for the determination of specific molecular markers of biomass burning in lake sediments. *Org. Geochem.* **71**, 1–6 (2014).
47. Suciu, L. G., Masiello, C. A. & Griffin, R. J. Anhydrosugars as tracers in the Earth system. *Biogeochemistry* **146**, 209–256 (2019).
48. Kuo, L. J., Louchouarn, P. & Herbert, B. E. Influence of combustion conditions on yields of solvent-extractable anhydrosugars and lignin phenols in chars: implications for characterizations of biomass combustion residues. *Chemosphere* **85**, 797–805 (2011).
49. Simoneit, B. R. T. Biomass burning—a review of organic tracers for smoke from incomplete combustion. *Appl. Geochem.* **17**, 129–162 (2002).
50. Aichner, B. et al. Hydroclimate in the Pamirs was driven by changes in precipitation-evaporation seasonality since the last glacial period. *Geophys. Res. Lett.* **46**, 13972–13983 (2019).
51. Wilkie, K. M. K., Chapligin, B., Meyer, H., Burns, S., Petsch, S. & Brigham-Grette, J. Modern isotope hydrology and controls on delta D of plant leaf waxes at Lake El'gygytgyn, NE Russia. *Clim. Past* **9**, 335–352 (2013).
52. Rao, Z. G. et al. Asynchronous evolution of the isotopic composition and amount of precipitation in north China during the Holocene revealed by a record of compound-specific carbon and hydrogen isotopes of long-chain n-alkanes from an alpine lake. *Earth Planet. Sci. Lett.* **446**, 68–76 (2016).
53. Contreras-Rosales, L. A. et al. Evolution of the Indian Summer Monsoon and terrestrial vegetation in the Bengal region during the past 18 ka. *Quaternary Sci. Rev.* **102**, 133–148 (2014).
54. Rao, Z. G., Jia, G. D., Qiang, M. R. & Zhao, Y. Assessment of the difference between mid- and long chain compound specific delta Dn-alkanes values in lacustrine sediments as a paleoclimatic indicator. *Org. Geochem.* **76**, 104–117 (2014).
55. Hou, J. Z., D'Andrea, W. J., Wang, M. D., He, Y. & Liang, J. Influence of the Indian monsoon and the subtropical jet on climate change on the Tibetan Plateau since the late Pleistocene. *Quaternary Sci. Rev.* **163**, 84–94 (2017).
56. Thomas, E. K. et al. Changes in dominant moisture sources and the consequences for hydroclimate on the northeastern Tibetan Plateau during the past 32 kyr. *Quaternary Sci. Rev.* **131**, 157–167 (2016).
57. Cheng, H. et al. The climatic cyclicity in semiarid-arid central Asia over the past 500,000 years. *Geophys. Res. Lett.* **39**, L01705 (2012).
58. Liu, X. K. et al. New insights on Chinese cave delta O-18 records and their paleoclimatic significance. *Earth-Sci. Rev.* **207**, 103216 (2020).
59. Yang, X. L. et al. Early-Holocene monsoon instability and climatic optimum recorded by Chinese stalagmites. *Holocene* **29**, 1059–1067 (2019).
60. Bird, B. W. et al. A Tibetan lake sediment record of Holocene Indian summer monsoon variability. *Earth Planet Sci. Lett.* **399**, 92–102 (2014).
61. Yao, T. D. et al. A review of climate controls on delta O-18 in precipitation over the Tibetan Plateau: observations and simulations. *Rev. Geophys.* **51**, 525−548 (2013).
62. Long, H., Lai, Z., Fuchs, M., Zhang, J. & Li, Y. Timing of Late Quaternary palaeolake evolution in Tengger Desert of northern China and its possible forcing mechanisms. *Glob. Planetary Change* **92**−**93**, 119–129 (2012).
63. Herzschuh, U. et al. Position and orientation of the westerly jet determined Holocene rainfall patterns in China. *Nat. Commun.* **10**, 2376 (2019).
64. Pausata, F. S. R., Battisti, D. S., Nisancioglu, K. H. & Bitz, C. M. Chinese stalagmite delta O-18 controlled by changes in the Indian monsoon during a simulated Heinrich event. *Nat. Geosci.* **4**, 474–480 (2011).
65. Aichner, B., Herzschuh, U., Wilkes, H., Vieth, A. & Bohner, J. delta D values of n-alkanes in Tibetan lake sediments and aquatic macrophytes—a surface sediment study and application to a 16 ka record from Lake Koucha. *Org. Geochem.* **41**, 779–790 (2010).
66. Corcoran, M. C. et al. Hydrogen isotopic composition (delta H-2) of diatom-derived C-20 highly branched isoprenoids from lake sediments tracks lake water delta H-2. *Org. Geochem.* **150**, 104122 (2020).
67. Chivall, D. et al. Impact of salinity and growth phase on alkenone distributions in coastal haptophytes. *Org. Geochem.* **67**, 31–34 (2014).
68. Chivall, D. et al. The effects of growth phase and salinity on the hydrogen isotopic composition of alkenones produced by coastal haptophyte algae. *Geochim. Cosmochim. Acta* **140**, 381–390 (2014).
69. M'boule, D. et al. Salinity dependent hydrogen isotope fractionation in alkenones produced by coastal and open ocean haptophyte algae. *Geochim. Cosmochim. Acta* **130**, 126–135 (2014).
70. Schouten, S. et al. The effect of temperature, salinity, and growth rate on the stable hydrogen isotopic composition of long chain alkenones produced by Emiliania huxleyi and Gephyrocapsa oceanica. *Biogeosciences* **3**, 113–119 (2006).
71. van der Meer, M. T. J. et al. Hydrogen isotopic compositions of long-chain alkenones record freshwater flooding of the Eastern Mediterranean at the onset of sapropel deposition. *Earth Planet Sci. Lett.* **262**, 594–600 (2007).
72. van der Meer, M. T. J. et al. Large effect of irradiance on hydrogen isotope fractionation of alkenones in Emiliania huxleyi. *Geochim. Cosmochim. Acta* **160**, 16–24 (2015).
73. Weiss, G. M., Schouten, T., Damste, J. S. S. & van der Meer, M. T. J. Constraining the application of hydrogen isotopic composition of alkenones as a salinity proxy using marine surface sediments. *Geochim. Cosmochim. Acta* **250**, 34–48 (2019).
74. Longo, W. M. et al. Widespread occurrence of distinct alkenones from Group I haptophytes in freshwater lakes: Implications for paleotemperature and paleoenvironmental reconstructions. *Earth Planet Sci. Lett.* **492**, 239–250 (2018).
75. Cranwell, P. A. Long-chain unsaturated ketones in recent lacustrine sediments. *Geochim. Cosmochim. Acta* **49**, 1545–1551 (1985).
76. Chu, G. Q. et al. Long-chain alkenone distributions and temperature dependence in lacustrine surface sediments from China. *Geochim. Cosmochim. Acta* **69**, 4985–5003 (2005).
77. He, Y. X. et al. Late Holocene coupled moisture and temperature changes on the northern Tibetan Plateau. *Quaternary Sci. Rev.* **80**, 47–57 (2013).
78. Hou, J. Z. et al. Large Holocene summer temperature oscillations and impact on the peopling of the northeastern Tibetan Plateau. *Geophys. Res. Lett.* **43**, 1323–1330 (2016).
79. Liu, W. G., Liu, Z. H., Fu, M. Y. & An, Z. H. Distribution of the C-37 tetra-unsaturated alkenone in Lake Qinghai, China: a potential lake salinity indicator. *Geochim. Cosmochim. Acta* **72**, 988–997 (2008).
80. Liu, W. G. et al. Salinity control on long-chain alkenone distributions in lake surface waters and sediments of the northern Qinghai-Tibetan Plateau, China. *Geochim. Cosmochim. Acta* **75**, 1693–1703 (2011).
81. Sun, D., Chu, G. Q., Li, S. Q., Lu, C. F. & Zheng, M. P. Long-chain alkenones in sulfate lakes and its paleoclimatic implications. *Chinese Sci. Bull.* **49**, 2082–2086 (2004).
82. Wang, Z. & Liu, W. G. Calibration of the U (37) (K') index of long-chain alkenones with the in-situ water temperature in Lake Qinghai in the Tibetan Plateau. *Chinese Sci. Bull.* **58**, 803–808 (2013).
83. Zhao, C. et al. Holocene temperature fluctuations in the northern Tibetan Plateau. *Quaternary Res.* **80**, 55–65 (2013).
84. Zheng, Y. S., Huang, Y. S., Andersen, R. A. & Amaral-Zettler, L. A. Excluding the di-unsaturated alkenone in the U-37(K) index strengthens temperature

correlation for the common lacustrine and brackish-water haptophytes. *Geochim. Cosmochim. Acta* **175**, 36–46 (2016).
85. Brassell, S. C., Eglinton, G., Marlowe, I. T., Pflaumann, U. & Sarnthein, M. Molecular stratigraphy—a new tool for climatic assessment. *Nature* **320**, 129–133 (1986).
86. Prahl, F. G. & Wakeham, S. G. Calibration of unsaturation patterns in long-chain ketone compositions for paleotemperature assessment. *Nature* **330**, 367–369 (1987).
87. Pearson, E. J., Juggins, S. & Farrimond, P. Distribution and significance of long-chain alkenones as salinity and temperature indicators in Spanish saline lake sediments. *Geochim. Cosmochim. Acta* **72**, 4035–4046 (2008).
88. He, Y. X. et al. Appraisal of alkenone- and archaeal ether-based salinity indicators in mid-latitude Asian lakes. *Earth Planet Sci. Lett.* **538**, 116236 (2020).
89. Janssen, A. B. G. et al. Alternative stable states in large shallow lakes? *J Great Lakes Res.* **40**, 813–826 (2014).
90. Hilt, S., Henschke, I., Rucker, J. & Nixdorf, B. Can submerged macrophytes influence turbidity and trophic state in deep lakes? Suggestions from a case study. *J. Environ. Qual.* **39**, 725–733 (2010).
91. Sachse, R. et al. Extending one-dimensional models for deep lakes to simulate the impact of submerged macrophytes on water quality. *Environ. Modell Softw.* **61**, 410–423 (2014).
92. Aichner, B. et al. Ecological development of Lake Donggi Cona, north-eastern Tibetan Plateau, since the late glacial on basis of organic geochemical proxies and non-pollen palynomorphs. *Palaeogeogr. Palaeocl.* **313**, 140–149 (2012).
93. Rasmussen, S. O. et al. A stratigraphic framework for abrupt climatic changes during the Last Glacial period based on three synchronized Greenland ice-core records: refining and extending the INTIMATE event stratigraphy. *Quaternary Sci. Rev.* **106**, 14–28 (2014).
94. Saros, J. E. et al. Melting alpine glaciers enrich high-elevation lakes with reactive nitrogen. *Environ. Sci. Technol.* **44**, 4891–4896 (2010).
95. Hood, E., Battin, T. J., Fellman, J., O'Neel, S. & Spencer, R. G. M. Storage and release of organic carbon from glaciers and ice sheets. *Nat. Geosci.* **8**, 91–96 (2015).
96. Warner, K. A., Saros, J. E. & Simon, K. S. Nitrogen subsidies in glacial meltwater: implications for high elevation aquatic chains. *Water Resour. Res.* **53**, 9791–9806 (2017).
97. Zhao, Y. & Yu, Z. C. Vegetation response to Holocene climate change in East Asian monsoon-margin region. *Earth-Sci. Rev.* **113**, 1–10 (2012).
98. Blaauw, M. & Christen, J. A. Flexible paleoclimate age-depth models using an autoregressive gamma process. *Bayesian Anal.* **6**, 457–474 (2011).
99. Rach, O., Hadeen, X. & Sachse, D. An automated solid phase extraction procedure for lipid biomarker purification and stable isotope analysis. *Org. Geochem.* **142**, 103995 (2020).
100. Kandiano, E. S. et al. Response of the North Atlantic surface and intermediate ocean structure to climate warming of MIS 11. *Sci. Rep.* **7**, 46192 (2017).
101. Aichner, B. et al. Concentrations and δD values of biomarkers in sediment cores H7 and H11 from Hala Hu, China. *PANGAEA* https://doi.org/10.1594/PANGAEA.933814 (2021).
102. Ramisch, A. et al. A persistent northern boundary of Indian Summer Monsoon precipitation over Central Asia during the Holocene. *Sci. Rep.* **6**, 25791 (2016).
103. Berger, A. & Loutre, M. F. Insolation values for the climate of the last 10000000 years. *Quaternary Sci. Rev.* **10**, 297–317 (1991).
104. Dykoski, C. A. et al. A high-resolution, absolute-dated Holocene and deglacial Asian monsoon record from Dongge Cave, China. *Earth Planet Sci. Lett.* **233**, 71–86 (2005).
105. Wang, Y. J. et al. A high-resolution absolute-dated Late Pleistocene monsoon record from Hulu Cave, China. *Science* **294**, 2345–2348 (2001).
106. Wang, Y. J. et al. The Holocene Asian monsoon: links to solar changes and North Atlantic climate. *Science* **308**, 854–857 (2005).
107. Liu, W. G. & Huang, Y. S. Compound specific D/H ratios and molecular distributions of higher plant leaf waxes as novel pale oenvironmental indicators in the Chinese Loess Plateau. *Org. Geochem.* **36**, 851–860 (2005).
108. Saini, J. et al. Climate variability in the past similar to 19,000 yr in NE Tibetan Plateau inferred from biomarker and stable isotope records of Lake Donggi Cona. *Quaternary Sci. Rev.* **157**, 129–140 (2017).
109. Gunther, F. et al. Quaternary ecological responses and impacts of the Indian Ocean Summer Monsoon at Nam Co, Southern Tibetan Plateau. *Quaternary Sci. Rev.* **112**, 66–77 (2015).

Acknowledgements

We thank the German Research Foundation for funding of projects Ai 134/2-1 and 2-2, WU 270-10/3, and Priority Programme 1372. Further we acknowledge the National Science Foundation of China (grant nos. 40971003 and 41806105) and the "Ideas" Specific Programme of the European Research Council (Advanced Grant 2010, grant agreement no. 267696). We are grateful to three anonymous reviewers and to Melissa Berke for providing valuable constructive comments which lead to significant improvement of the manuscript.

Author contributions

B.A. analyzed organic geochemical parameters in the organic surface geochemistry lab of D.S. at GFZ Potsdam and wrote the manuscript. A.C. analyzed firemarkers in the lab of C.B. at University of Venice. M.v.M. analyzed δD values of alkenones in the NIOZ labs. B.W., D.Y., and Y.Z. provided the samples. All co-authors contributed to the discussion of results and the manuscript draft.

Funding

Open Access funding enabled and organized by Projekt DEAL.

Competing interests

The authors declare no competing interests.

Additional information

Supplementary information The online version contains supplementary material available at https://doi.org/10.1038/s43247-021-00325-1.

Correspondence and requests for materials should be addressed to Bernhard Aichner.

Peer review information *Communications Earth & Environment* thanks Michael Hren and the other, anonymous, reviewer(s) for their contribution to the peer review of this work. Primary Handling Editors: Sze Ling Ho and Clare Davis. Peer reviewer reports are available.

Reprints and permission information is available at http://www.nature.com/reprints

Publisher's note Springer Nature remains neutral with regard to jurisdictional claims in published maps and institutional affiliations.